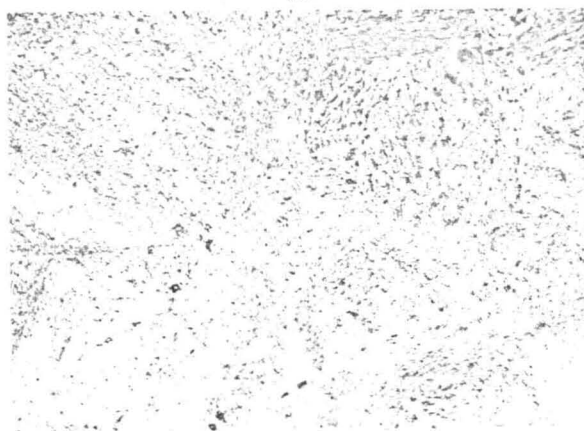
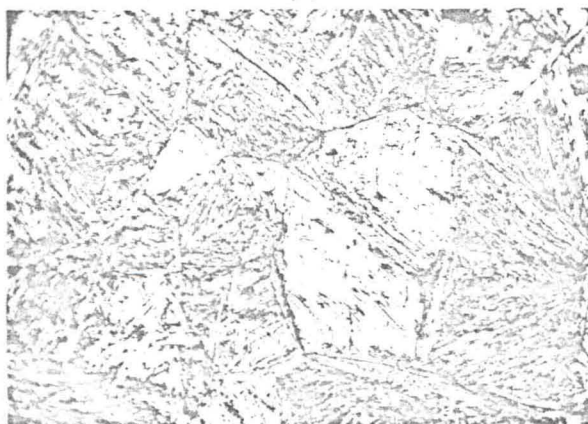


(a)



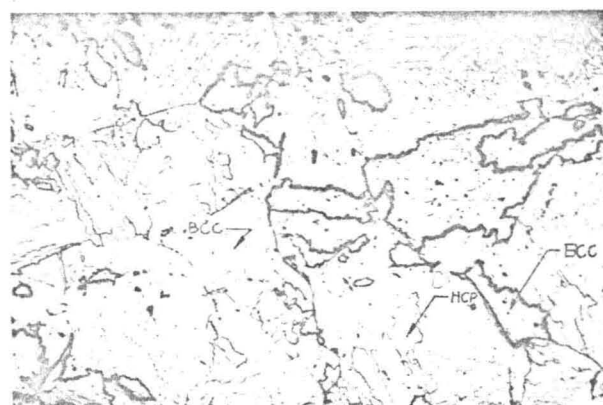
(b)



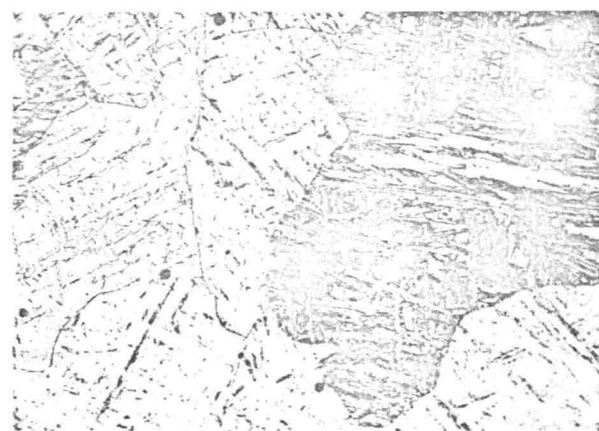
(c)

FIG. 4. (a) Typical Fe-Mn unshocked microstructure following a water quench. Magnification is 500 \times . Austenitic grain boundaries are hidden. (b) Shock-loaded Fe-7Mn at 300 kbar, showing mixed microstructure. Austenitic grain boundaries have reappeared due to the retainment of the high-pressure fcc phase. Magnification is 500 \times . (c) Microstructure of the shocked Fe-7Mn. Typical martensitic structure is shown, with prior austenitic grain boundaries. Magnification is 500 \times .

specimens clearly indicate that the high-pressure phase has been retained in the alloys Fe-4Mn to Fe-14Mn, which were shock loaded at pressures above 90 kbar. The maximum density change occurred after shock deformation at 300 kbar for Fe, Fe-0.4Mn, and Fe-4Mn and at 500 kbar for Fe-7Mn and Fe-



(a)



(b)

FIG. 5. (a) Microstructure of Fe-7Mn slow cooled from 900 $^{\circ}$ C. The hcp phase is outlined by the lightly etched grain boundaries. The matrix is bcc. These observations have been verified by the electron probe. Magnification is 250 \times . (b) Microstructure of Fe-7Mn, slow cooled and shock loaded to 300 kbar. Profuse twinning is evident. Magnification is 500 \times .

14Mn. From 300–500 kbar there was no appreciable change in the retention of the close-packed phases. No appreciable density changes were observed in the Fe and Fe-0.4Mn alloys. The density change was much less in the alloys which were initially furnace cooled prior to shock deformation. The residual density changes are believed to be due to an $\alpha' \rightarrow \gamma$ or $\alpha' \rightarrow \epsilon$ transformation. The stability of the shock-